

Machining and Phase Transformation Response of Room-Temperature Austenitic NiTi Shape Memory Alloy

Yusuf Kaynak

(Submitted February 3, 2014; in revised form April 23, 2014; published online June 14, 2014)

This experimental work reports the results of a study addressing tool wear, surface topography, and x-ray diffraction analysis for the finish cutting process of room-temperature austenitic NiTi alloy. Turning operation of NiTi alloy was conducted under dry, minimum quantity lubrication (MQL) and cryogenic cooling conditions at various cutting speeds. Findings revealed that cryogenic machining substantially reduced tool wear and improved surface topography and quality of the finished parts in comparison with the other two approaches. Phase transformation on the surface of work material was not observed after dry and MQL machining, but B19' martensite phase was found on the surface of cryogenically machined samples.

Keywords cryogenic and MQL machining, phase transformation, room-temperature austenitic NiTi alloy, tool wear, XRD analysis

1. Introduction

NiTi shape memory alloys have attracted considerable attention in their use with medical implants (Ref 1) due to unique thermo-mechanical properties—namely, shape memory, superelasticity, good biocompatibility, and corrosion resistance (Ref 2). Improved machined tools and manufacturing approaches allow utilization of machining as a finish process to fabricate components used in various industries including biomedical industries.

One of the challenges of NiTi alloy machining is extremely poor machinability with rapid and uncontrollable tool wear and poor surface quality of machined parts due to high ductility, superelasticity, low elastic modulus, work hardening, etc. (Ref 3-5). Although some studies have made efforts to improve machining performance of martensitic NiTi alloys by proposing cryogenic machining to reduce progressive tool wear, and improve surface quality (Ref 5), the deformation response of NiTi alloys strongly depends on active phase during the cutting process and room-temperature phase. Further investigation that considers austenitic phases is needed to observe whether or not cryogenic machining is effective in reducing tool wear in machining austenitic shape memory alloys.

It has been clearly documented that machining process has considerable effects on surface, subsurface, and functional performance of machined parts (Ref 6-9). In addition to improving machining performance by reducing tool wear and improving machined parts' quality, examination of shape

memory properties or phase state of machined parts is necessary for this particular alloy. Several attempts have been made to understand the effects of conventional cutting on microhardness of work materials' subsurface, microstructure, and deformation response in drilling (Ref 4), milling (Ref 10), and orthogonal cutting process (Ref 11).

In addition to using conventional cutting fluids, investigating the effects of different cooling/lubricating is particularly important in machining shape memory alloys that have relatively low phase transformation temperature. Thermo-mechanical and deformation response of these alloys depends on temperature. Consequently, using cooling in the cutting process of this alloy is expected to influence the machining performance of these alloys. Cryogenic cooling, as an emerging approach utilized in machining community, (Ref 12-15) needs to be considered for its contribution to machining performance and product quality and integrity.

Three main points need to be addressed to propose conventional SMA machining process as an alternative: cutting tool performance, surface quality of machined NiTi alloys, and whether or not machining-induced phase transformation occurs. In this study, the effect of cooling/lubricating and various cutting speeds on tool wear and surface quality in machining room-temperature austenitic NiTi alloy was determined by utilizing dry, MQL, and cryogenic cooling. The influences of cooling/lubricating and various cutting speeds on XRD pattern and phase state of machined parts were also presented.

2. Experimental Procedure

The work material used in this study was vacuum arc remelting (VAR) melted and hot rolled followed by a full anneal condition with a diameter of 12.5 mm. To examine microstructure of the as-received specimen, 3.2 vol.% HF + 14.6 vol.% HNO₃ + 82.2 vol.% H₂O was used as the etchant after the cold mounting, grinding, and polishing processes. The cross-sectional microstructure of specimens was examined by a digital optical microscopy (Keyence

Yusuf Kaynak, Department of Mechanical Engineering, Faculty of Technology, Marmara University, Goztepe Campus, 34722 Kadikoy, Istanbul, Turkey. Contact e-mails: yusuf_kaynak@yahoo.com and yusuf.kaynak@marmara.edu.tr.

VHX-1000 HDR) and average grain size was measured to be approximately $67 \pm 10 \mu\text{m}$. The microstructure of the as-received material is presented in Fig. 1. Phase transformation temperatures for martensite start (M_s), martensite finish (M_f), austenite start (A_s), and austenite finish (A_f), all in $^{\circ}\text{C}$, were measured as -43 , -71 , -32 , and -11 , respectively, by differential scanning calorimetry (DSC).

A DCGT11T308HP grade KC5410 cutting tool insert with TiB2 coating was used in these experiments with the edge radius of the tools varying between 18 and $20 \mu\text{m}$. This selected insert with coating is a commonly used tool type in industry for the turning of NiTi shape memory alloys (Ref 5). The tool holder was an SDJCL123BH5 M. The cutting experiments were conducted on a Mazak CNC lathe. During the machining tests, based on experience (Ref 5) and industry recommendations, a constant feed rate, $f = 0.05 \text{ mm/rev}$; constant depth of cut, $d = 0.5 \text{ mm}$; and various cutting speeds, $V = 12.5$, 25 , and 50 m/min , were used. The cutting length for each test was 25 mm . The cryogenic coolant was liquid nitrogen, which was applied under 1.5 MPa pressure, and approximately 10 g/s mass flow rate. Liquid nitrogen was delivered to the cutting region through two 4.78-mm -diameter nozzles. One nozzle was placed on the rake face of the cutting tool; while the other nozzle was placed on the back of the tool holder to deliver liquid nitrogen toward the cutting tool tip, making an approximately 55° angle with the rake face of the cutting tool (Ref 5). For minimum quantity lubrication (MQL), a UNIST system with Coolube 2210EP metalworking lubricant was used at a flow rate of 60 ml/h , and approximately 0.4 MPa air pressure. MQL was applied at the rake face region of the tool. Tool wear was measured using a digital optical microscope, and surface roughness and topography were measured using an interferometry optical profiler ZYGO 3D-New View 7300.

To analyze the phase transformation of the as-received and machined NiTi samples, x-ray diffractometer, XRD BrukerD8 Discover with a quarter Eulerian cradle that integrates phi and chi rotations, was used. The x-ray diffraction (XRD) patterns were measured using $\text{CuK}\alpha$ radiation ($\lambda = 1.5406 \text{ \AA}$ -nm, $\text{K}\alpha_1/\text{K}\alpha_2 = 0.5$) from a source operated at 40 kV and 44 mA . The round bar samples were positioned at the center of the x-ray goniometer. XRD spectra of machined NiTi samples were carried out within the ranging of 35 to 50 degree 2θ scans at room temperature. The scan speed was 1.5 deg/min .

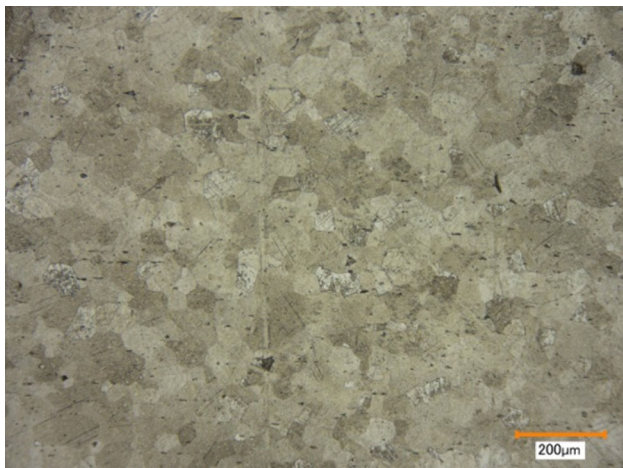


Fig. 1 Cross section microstructure of room-temperature austenitic NiTi alloy

3. Results and Discussion

3.1 Tool Wear

An important goal in machining difficult-to-machine materials is to improve tool performance to achieve high machining performance. This section addresses the role of cutting speed and cooling/lubricating on tool wear response in machining this particular alloy. Due to the depth of cut normally being less than the radius of the tool nose in finish operations, the maximum flank wear land width measured at the major flank face is not a suitable criterion for evaluating the tool wear. As a result, the flank wear land in the nose area, or just called “nose wear,” is a more meaningful parameter for assessing tool wear (Ref 16). Typical nose wear (VB_C) is schematically illustrated in Fig. 2. Figure 3 shows tool wear in machining process of this alloy under different machining conditions (dry, MQL, and cryogenic) and cutting speeds. The greatest nose wear was observed in dry machining among all three conditions at various cutting speeds. Cryogenic machining shows excellent performance by substantially reducing nose wear at all three cutting speeds. Although MQL machining contributed to reduced nose wear at lower cutting speed, it did not assist in controlling nose wear at the highest cutting speed, 50 m/min . Extremely high nose wear followed by chipping (flaking) was observed in dry and MQL machining at 50 m/min cutting speed; therefore, it is difficult to find the exact value of nose wear in those conditions. Even before chipping, large tool wear on the nose region existed. All three conditions can be compared at 25 m/min cutting speed. At 25 m/min cutting speed, nose wear was approximately 72 , 140 , and $250 \mu\text{m}$ in cryogenic, MQL, and dry machining, respectively. Quantitative comparison of measured nose wear in these conditions and various cutting speeds is presented in Fig. 4. Due to flaking in

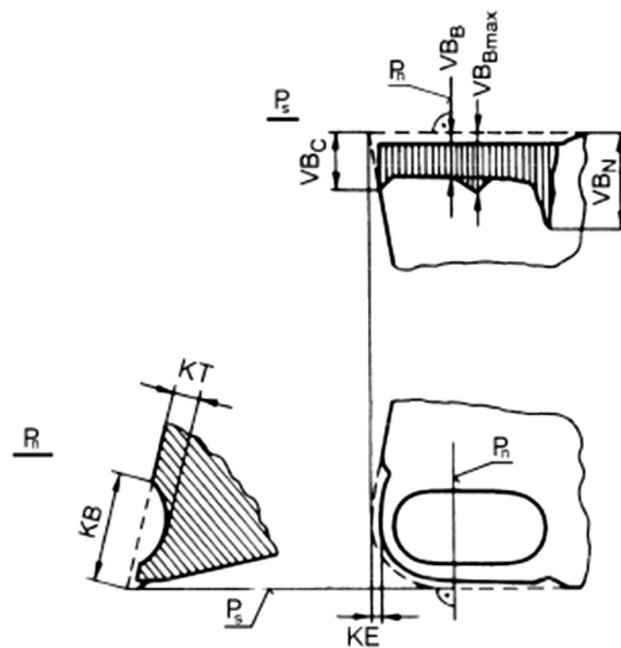


Fig. 2 Typical features of turning tool wear: flank wear land length (VB_B), nose wear land length (VB_C), notch wear (VB_C), and distance between the primary cutting edge and the most distant crater (KB), tip wear (KE), and crater depth (KT). Units in mm or μm (Ref 26)

dry and MQL at the highest cutting speed, measurement was not possible and those conditions are not presented in Fig. 4.

Deep grooves on the nose region of the cutting tool indicate abrasive wear. It is obvious that in machining these alloys, extremely high abrasive wear was observed on the nose region of cutting tools in all three conditions with given cutting speeds. In review of the literature, abrasive wear is a dominant wear mechanism in machining martensitic NiTi alloy (Ref 5). This current study shows that in machining of room-temperature austenitic NiTi alloy, similar wear mechanism is observed. When the cutting tools are examined from the rake face, shown in Fig. 5, it can be seen that chipping also occurs on the rake face of cutting tools under some conditions. In dry and MQL machining, increased cutting speed leads to chipping failure on the rake face of cutting tools. The effect of cooling on reduced tool wear is evident considering the obtained results at all cutting speeds with cryogenic machining (shown in Fig. 3). The current findings in this study agree with previous studies, where cryogenic machining decreases tool wear in the machining process of various work materials due to low temperature (Ref 17-20).

3.2 Surface Roughness and Quality of Work Material

Improving surface quality of machined NiTi alloys is also needed to fabricate components used in biomedical industry. Indeed, product surface quality in this industry is very important if components are implants. Surface topographies

of the machined samples under dry, MQL, and cryogenic conditions at the lowest cutting speed ($V = 12.5$ m/min) and the highest cutting speed ($V = 50$ m/min) are shown in Fig. 6. Debris on the machined surface in dry cutting at the lowest cutting speed was observed, which led to increased surface roughness. Under the dry machining condition, large differences were observed between peak and valley on feed marks of the machined surface at the highest cutting speed. In addition, scratches and local deformation on the surface due to tool wear were also seen on dry-machined sample, which resulted in increased surface roughness. At the lowest cutting speed,

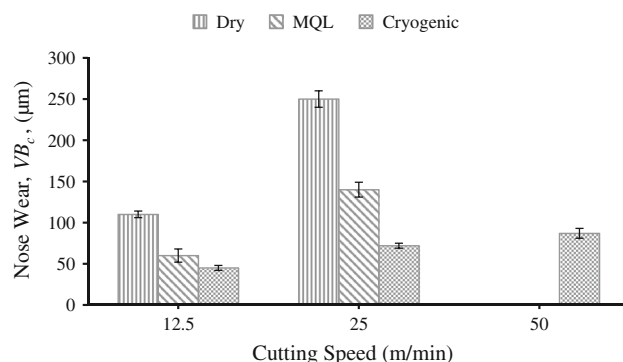


Fig. 4 Nose wear as a function of various cutting speeds under dry, MQL, and cryogenic machining

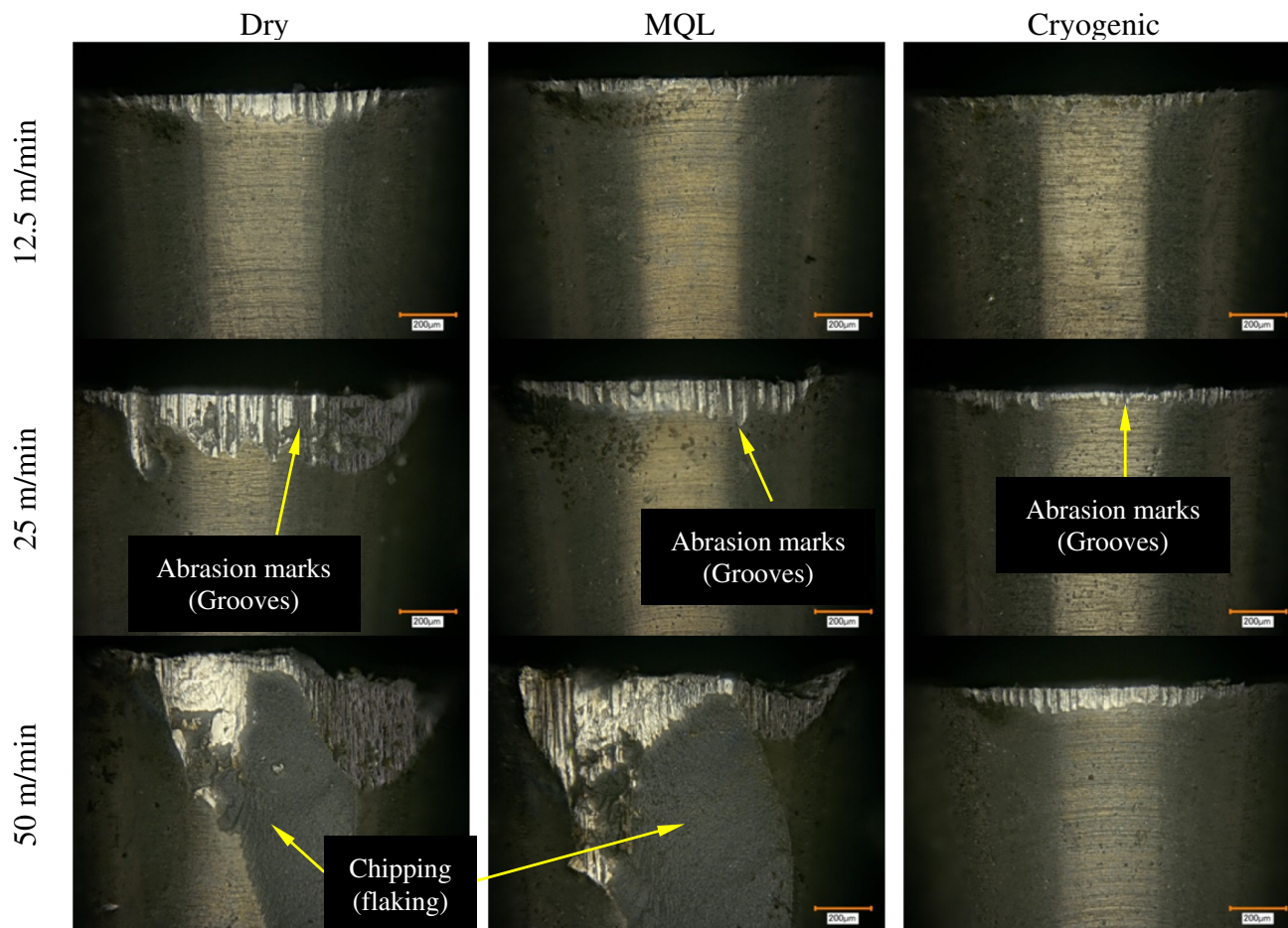


Fig. 3 Tool wear at nose region in machining of room-temperature austenitic NiTi alloys

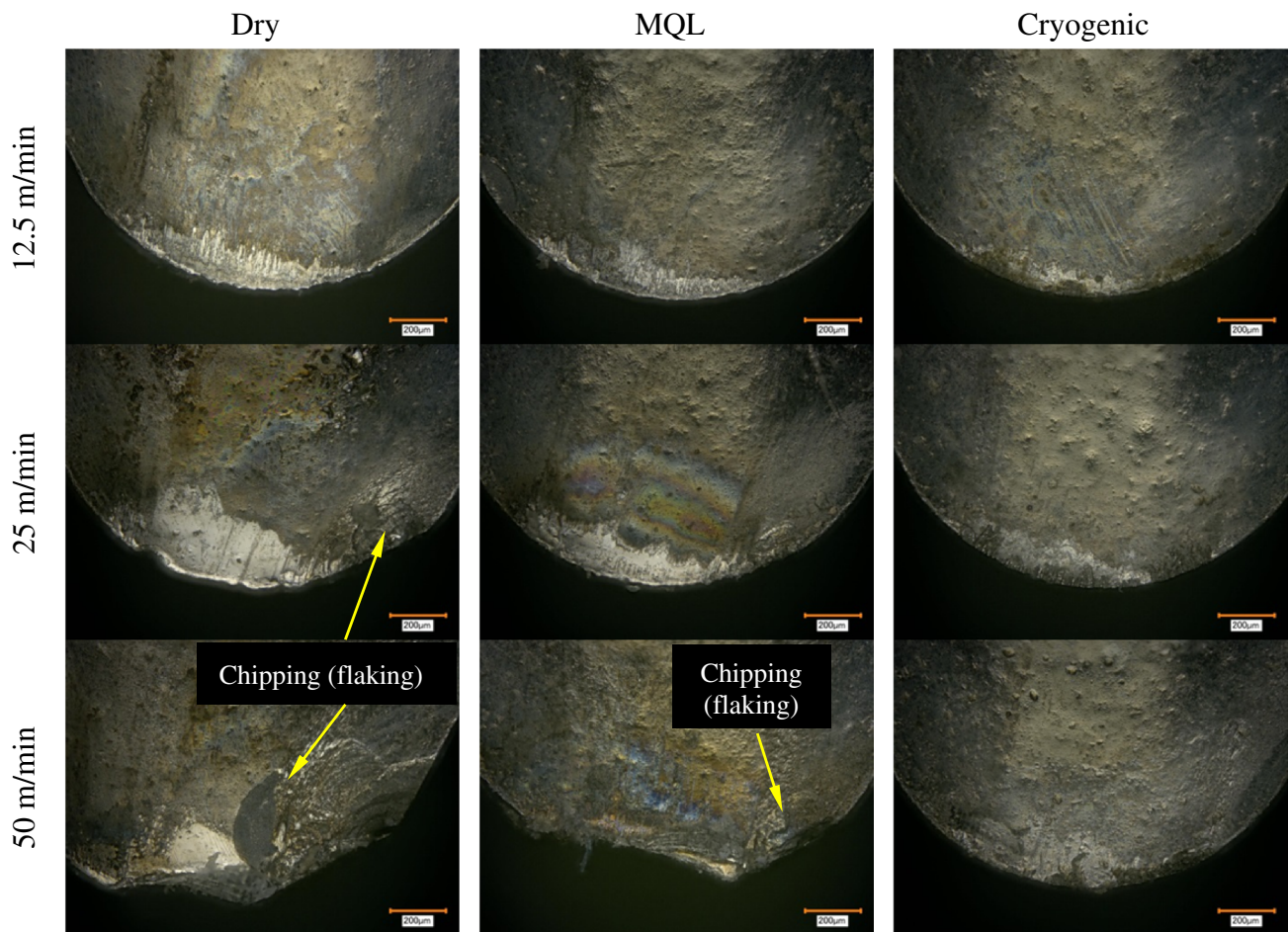


Fig. 5 Tool wear at rake face of cutting tool in machining of room-temperature austenitic NiTi alloys

surface topography of the machined sample under the MQL condition did not generate any clear surface defects. Smooth and consistent surface was observed. However, when cutting speed increased, inconsistent feed marks with big peak and valley, as seen in Fig. 6, resulted in increased surface roughness. This roughness is attributed to increased nose wear at high cutting speed. Cryogenic machining at low and high cutting speeds generated consistent and smooth surface topography, which resulted in less surface roughness compared to dry and MQL machining. In terms of surface quality, the difference between cryogenic approach and the other two approaches was seen at the highest cutting speed. Although MQL generated the best surface quality at the lowest cutting speed, cryogenic machining produced the best surface topography and quality between all three conditions at the highest cutting speed due to reduced tool wear and much lower temperature at the interface between the cutting tool and the work material.

The quantitative measurements of surface roughness of machined samples are presented in Fig. 7. MQL and cryogenic machining generated a surface roughness value of approximately $0.2 \mu\text{m}$. Increased cutting speed resulted in increased surface roughness in all three conditions. In finish-machining process, the expected surface roughness value is approximately $0.75 \mu\text{m}$ (Ref 21). Depending on the application, the expected value might be necessary to produce much better surface. In considering $0.75 \mu\text{m}$ as a reference value, cryogenic machining

generated surface roughness values much lower than $0.75 \mu\text{m}$. In MQL machining, surface quality demand was also met with the exception for the highest cutting speed conditions.

Overall, it is evident that in machining room-temperature austenitic NiTi alloy, cryogenic machining meets the requirement of surface quality for finish machining even at higher cutting speed. At lower cutting speed, MQL demonstrated very good performance and substantially reduced surface roughness.

3.3 XRD and Phase Transformation Analysis

Compared to many engineering materials, NiTi shape memory alloys have relatively low phase transformation temperature. During machining process, the generated heat resulting in high temperature coupled with high stress may affect the active phase of the work material. Altered phase of work material may then result in altered thermal and mechanical properties on the surface and subsurface of machined shape memory alloys. Consequently, examining the phase state of the machined surface of the work material is necessary. In this study, qualitative analysis to determine the phase state of the machined samples is presented. Figure 8 shows the XRD pattern of the as-received and dry-machined samples at different cutting speeds. The XRD pattern of the as-received sample shows only the B2 diffraction peak with (1 1 0) Miller index. Dry machined samples have the same diffraction peak

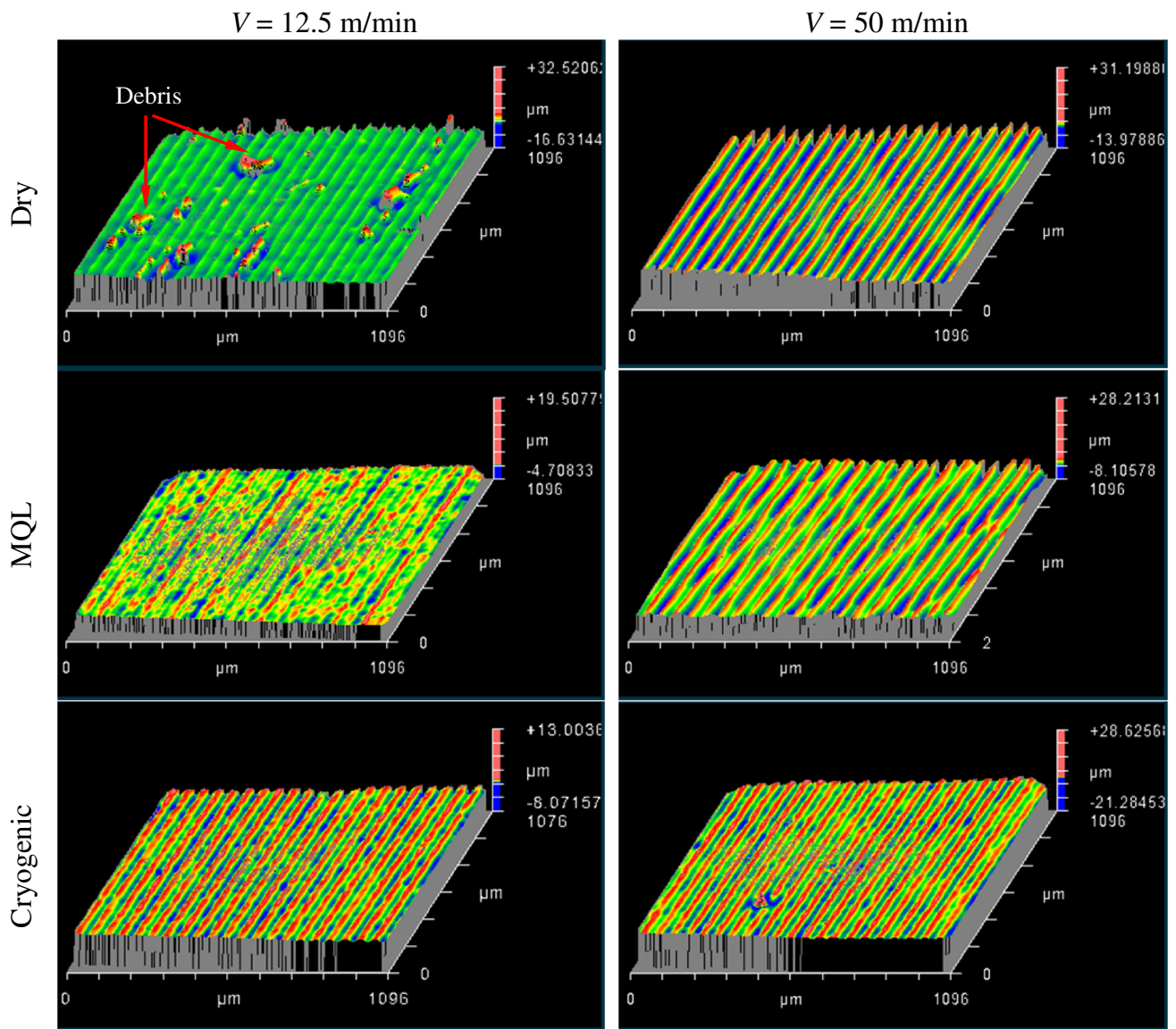


Fig. 6 Surface topography of the machined samples

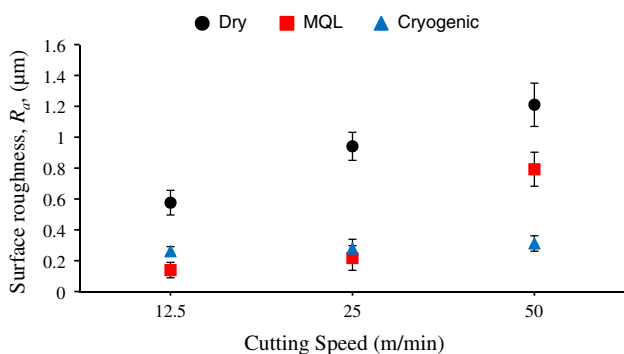


Fig. 7 Measured average surface roughness of the machined samples

within the presented range of diffraction angle. As cutting speed decreased the peak broadened. At the lowest cutting speed, the broadest peak was obtained. Similarly, at the highest

cutting speed conditions, the narrowest peak was observed. Relative intensity was not significantly affected by cutting speed. Figure 8 illustrates that machining results in broader peak compared to the as-received material regardless of the cutting conditions.

Similar to dry-machined samples, MQL-machined samples also showed one diffraction peak B2, as displayed in Fig. 9. As cutting speed decreased the peak became broader. At lower cutting speed, cutting temperature was relatively lower than that under the high cutting speed due to low strain rate (Ref 22). Consequently, the mechanical effect was more dominant compared to the thermal effect (Ref 23) leading to increased dislocation density and defects in microstructure of the machined surface. As a result peak broadening was observed. Increased cutting temperature, from higher cutting speed and larger tool wear, annihilates the mechanical effect of deformation by reducing dislocation density and stress. Consequently, diffraction peaks obtained from samples machined at higher cutting speed do not show considerable peak broadening.

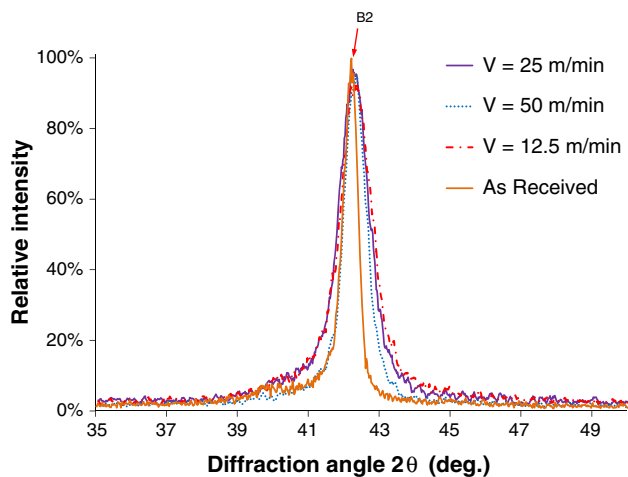


Fig. 8 XRD patterns of machined room-temperature austenitic NiTi alloy with dry machining condition

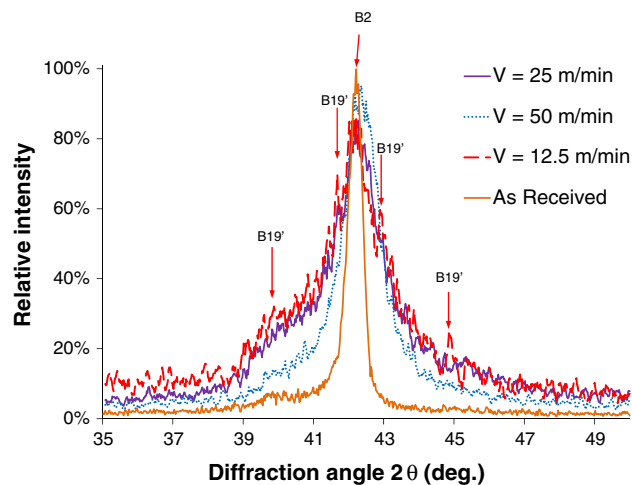


Fig. 10 XRD patterns of machined room-temperature austenitic NiTi alloy with cryogenic machining condition

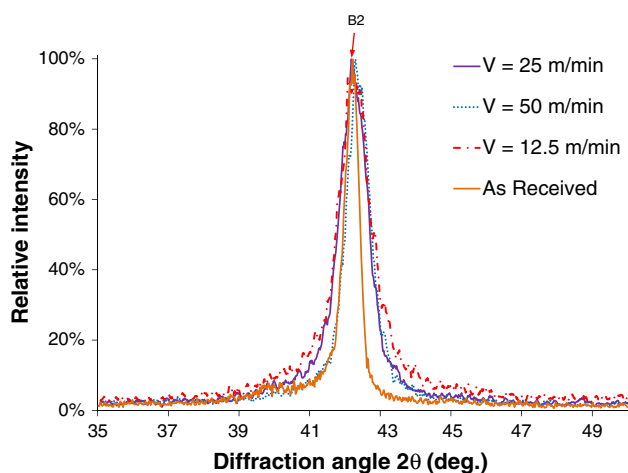


Fig. 9 XRD patterns of machined room-temperature austenitic NiTi alloy with MQL machining condition

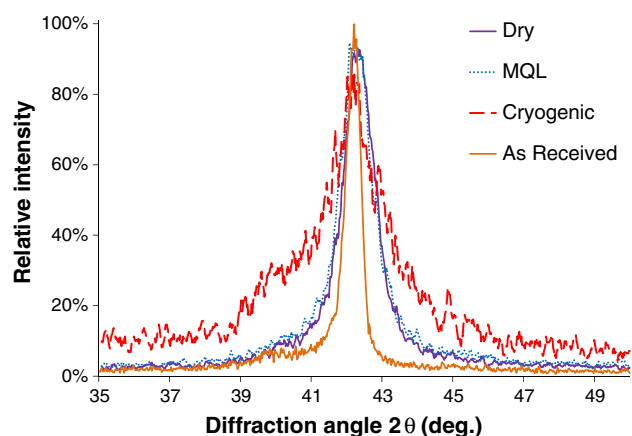


Fig. 11 Comparison of XRD patterns of dry, MQL, and cryogenic conditions at 12.5 m/min cutting speed

Figure 9 also supports the argument that machined samples generate broadened peaks compared to the as-received material.

Figure 10 shows the XRD patterns of the as-received and cryogenically machined samples at different cutting speeds. Although the main diffraction peak is B2 in cryogenically machined samples, B19' martensitic peaks were also observed at lower cutting speeds. These peaks indicate that local martensitic structure took place after cryogenic machining process.

During cryogenic machining, liquid nitrogen was delivered to the deformation region resulting in substantially reduced temperature. Martensite start (M_s) temperature of this NiTi alloy was $-43\text{ }^\circ\text{C}$. Considering cryogenic temperature, at low cutting speed, the work material was machined while it was either partially or fully in martensite phase state depending on the temperature. Due to the stress introduced to the surface and subsurface during severe deformation process, fully reverse phase transformation ($M \rightarrow A$) did not take place. For this reason, B19' diffraction peaks were observed. At the highest cutting speed, B19' was not observed because of the high cutting speed and the associated high temperature. Significant peak broadening with cryogenically machined sample was also observed compared to the as-received material, as shown in Fig. 10.

Figure 11 shows comparisons of the XRD pattern of dry, MQL, and cryogenically machined sample at 12.5 m/min cutting speed and the as-received sample's XRD pattern. It is evident that cryogenically machined sample showed the broadest peak compared to other conditions. In addition, cryogenically machined sample also showed martensitic peaks. XRD patterns of the as-received and machined samples at high cutting speed (50 m/min) are illustrated in Fig. 12. Similar to the low cutting speed, cryogenic machining compared with other conditions generates the broadest peak at high cutting speed. This indicates that cutting this material at lower temperature broadened the XRD peaks. Findings presented in this study concur with previous studies where it was noted that cold work results in peak broadening (Ref 24, 25).

4. Conclusions

The current study demonstrates that cryogenic machining improves cutting tool performance in machining room-temperature austenitic NiTi shape memory alloy. In addition, cryogenic machining generated much better surface quality

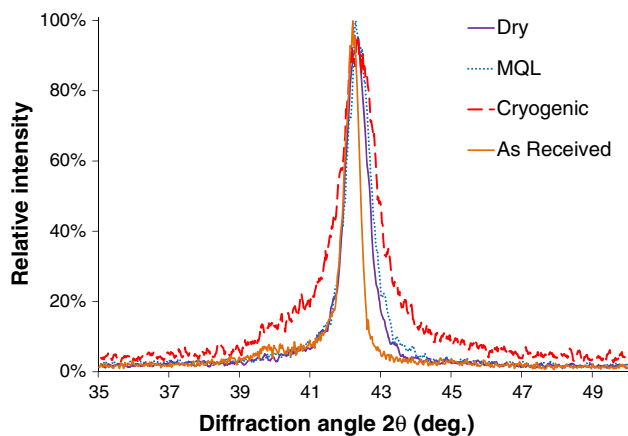


Fig. 12 Comparison of XRD patterns of dry, MQL, and cryogenic conditions at 50 m/min cutting speed

compared to dry and MQL machining. While the phase state of the machined surface of NiTi alloy remained the same as austenite (B2) state during dry and MQL machining, martensite phase (B19') was observed on cryogenically machined surface of samples at low cutting speeds. With consideration of biomedical industrial applications of these room-temperature austenitic NiTi alloys, cryogenic machining is highly recommended for improving machinability of room-temperature austenitic NiTi alloys. However, it is also important to consider that the surface phase state of the machined samples is altered with cryogenic machining.

Acknowledgments

The author would like to offer sincere thanks to Prof. I.S. Jawahir and the Institute for Sustainable Manufacturing (ISM) for providing test equipments for this study. The author would like to thank Dr. S.W. Robertson from Nitinol Devices & Components, Inc. for providing work materials for this study. Additionally, gratitude is extended to Doc. Dr. M. Kemal Ozturk from Gazi University for providing XRD equipment.

References

1. T. Duerig, A. Pelton, and D. Stockel, *An Overview of Nitinol Medical Applications*, Elsevier Science, Oxford, 1999, p 149–160
2. B. Thierry, M. Tabrizian, C. Trepanier, O. Savadogo, and L.H. Yahia, Effect of Surface Treatment and Sterilization Processes on the Corrosion Behavior of NiTi Shape Memory Alloy, *J. Biomed. Mater. Res.*, 2000, **51**, p 685–693
3. K. Weinert, V. Petzoldt, and D. Kotter, Turning and Drilling of NiTi Shape Memory Alloys, *CIRP Ann. Manuf. Technol.*, 2004, **53**, p 65–68
4. K. Weinert and V. Petzoldt, Machining of NiTi Based Shape Memory Alloys, *Mater. Sci. Eng.*, 2004, **A378**, p 180–184
5. Y. Kaynak, H.E. Karaca, R.D. Noebe, and I.S. Jawahir, Tool-Wear Analysis in Cryogenic Machining of NiTi Shape Memory Alloys: A Comparison of Tool-Wear Performance with Dry and MQL Machining, *Wear*, 2013, **306**, p 51–63
6. I.S. Jawahir, E. Brinksmeier, R. M'Saoubi, D.K. Aspinwall, J.C. Quteiro, D. Meyer, D. Umbrello, and A.D. Jayal, Surface Integrity in Material Removal Processes: Recent Advances, *CIRP Ann. Manuf. Technol.*, 2011, **60**, p 603–626
7. R. M'Saoubi, J. Outeiro, H. Chandrasekaran, O. Dillon, Jr., and I.S. Jawahir, A Review of Surface Integrity in Machining and its Impact on Functional Performance and Life of Machined Products, *Int. J. Sustain. Manuf.*, 2008, **1**, p 203–236
8. J. Outeiro, J. Pina, R. M'saoubi, F. Pusavec, and I.S. Jawahir, Analysis of Residual Stresses Induced by Dry Turning of Difficult-to-Machine Materials, *CIRP Ann. Manuf. Technol.*, 2008, **57**, p 77–80
9. A. Jayal, F. Badurdeen, O. Dillon, Jr., and I.S. Jawahir, Sustainable Manufacturing: Modeling and Optimization Challenges at the Product, Process and System Levels, *CIRP J. Manuf. Sci. Technol.*, 2010, **2**, p 144–152
10. Y. Guo, A. Klink, C. Fu, and J. Snyder, Machinability and Surface Integrity of Nitinol Shape Memory Alloy, *CIRP Ann. Manuf. Technol.*, 2013, **62**, p 83–86
11. Y. Kaynak, H. Tobe, R.D. Noebe, H. Karaca, and I.S. Jawahir, The Effects of Machining on Microstructure and Transformation Behavior of NiTi Alloy, *Scr. Mater.*, 2014, **74**, p 60–63
12. F. Pusavec, H. Hamdi, J. Kopac, and I.S. Jawahir, Surface Integrity in Cryogenic Machining of Nickel Based Alloy—Inconel 718, *J. Mater. Process. Technol.*, 2011, **211**, p 773–783
13. Y. Kaynak, H. Karaca, I.S. Jawahir, Cryogenic Machining of NiTi Shape Memory Alloy, *6th Int. Conference and Exhibition on Design and Production of Machines and Dies/Molds*, 2011, p 23–26
14. Z.Y. Wang, K.P. Rajurkar, Cryogenic machining of hard-to-cut materials, *Wear*, 2000, **239**, p 168–175
15. S.Y. Hong, I. Markus, W. Jeong, New cooling approach and tool life improvement in cryogenic machining of titanium alloy Ti-6Al-4V, *Int. J. Mach. Tool. Manu.*, 2001, **41**, p 2245–2260
16. H. Shahabi and M. Ratnam, Assessment of Flank Wear and Nose Radius Wear from Workpiece Roughness Profile in Turning Operation Using Machine Vision, *Int. J. Adv. Manuf. Technol.*, 2009, **43**, p 11–21
17. Y. Kaynak, Evaluation of Machining Performance in Cryogenic Machining of Inconel 718 and Comparison with Dry and MQL Machining, *Int. J. Adv. Manuf. Technol.*, 2014, **72**, p 919–933
18. Y. Kaynak, H.E. Karaca, R.D. Noebe, and I.S. Jawahir, Analysis of Tool-Wear and Cutting Force Components in Dry, Preheated, and Cryogenic Machining of NiTi Shape Memory Alloys, *Proc. CIRP*, 2013, **8**, p 498–503
19. M. Bermingham, J. Kirsch, S. Sun, S. Palanisamy, and M. Dargusch, New Observations on Tool Life, Cutting Forces and Chip Morphology in Cryogenic Machining Ti-6Al-4V, *Int. J. Mach. Tools Manuf.*, 2011, **51**, p 500–511
20. K.A. Venugopal, S. Paul, and A.B. Chattopadhyay, Growth of Tool Wear in Turning of Ti-6Al-4V Alloy Under Cryogenic Cooling, *Wear*, 2007, **262**, p 1071–1078
21. M.C. Shaw, *Metal Cutting Principles*, Oxford Series on Advanced Manufacturing, 2nd ed., Oxford University Press, New York, 2005
22. Y. Kaynak, Process-Induced Surface Integrity in Machining of NiTi Shape Memory Alloys, University of Kentucky, Ph.D. dissertation, 2013
23. A. Ramesh, S. Melkote, L. Allard, L. Riester, and T. Watkins, Analysis of White Layers Formed in Hard Turning of AISI, 52100 Steel, *Mater. Sci. Eng.*, 2005, **A390**, p 88–97
24. M.E. Mitwally and M. Farag, Effect of Cold Work and Annealing on the Structure and Characteristics of NiTi Alloy, *Mater. Sci. Eng.*, 2009, **A519**, p 155–166
25. T. Hu, C. Wen, J. Lu, S. Wu, Y. Xin, W. Zhang, C. Chu, J. Chung, K. Yeung, and D. Kwok, Surface Mechanical Attrition Treatment Induced Phase Transformation Behavior in NiTi Shape Memory Alloy, *J. Alloys Compd.*, 2009, **482**, p 298–301
26. M. Szafarczyk and J. Chrzanowski, Tool Probe for Measuring Dimensional Wear and X-Coordinate of Turning Edge, *Int. J. Adv. Manuf. Technol.*, 2004, **23**, p 272–278